Archivos de Bronconeumología xxx (xxxx) xxx–xxx

separ
Sociedad Española de Neumología y Cirugía Torácica

ARCHIVOS DE
Bronconeumología

www.archbronconeumol.org

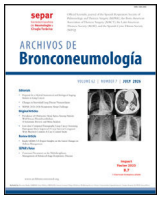

Original Article

Endothelial Cell Transcriptomics Reveal Activation of Ribosomal-related Pathways in Chronic Thromboembolic Pulmonary Hypertension

Míriam Peracaula[a,*], Daniel Aguilar[b], Àngela Vea[c], Cristina Rodríguez[c], Miquel Gratacós-Aurich[a,d], Júlia Cabrera-Serra[a], Jeisson Osorio[c,e], Isabel Blanco[c,f], Victor I. Peinado[c,e,f], Joan Carles Garcia-Pagan[g,h,i,j], Héctor García Calderó[g,h,i,j], Virginia Hernández Gea[g,h,i,j], Ana Paula Dantas[k], Maribel Diaz-Ricart[l,m], Fatima Crispi[n,o], Joan Albert Barberà[c,e,*], Olga Tura-Ceide[a,c,e,p,*]

[a] *Translational Research Group on Cardiovascular Respiratory Diseases (CAREs), Dr. Josep Trueta University Hospital de Girona, Santa Caterina Hospital de Salt and the Girona Biomedical Research Institute (IDIBGI-CERCA), 17190 Girona, Spain*
[b] *Centro de Investigación Biomédica en Red de Enfermedades Hepáticas y Digestivas (CIBEREHD), Barcelona, Spain*
[c] *Department of Pulmonary Medicine, Hospital Clínic-Institut d'Investigacions Biomèdiques August Pi I Sunyer (IDIBAPS), University of Barcelona, Villarroel, 170, 08036 Barcelona, Spain*
[d] *Department of Computer Sciences, Applied Mathematics and Statistics, University of Girona, Girona, Spain*
[e] *Biomedical Research Networking Centre on Respiratory Diseases (CIBERES), 28029 Madrid, Spain*
[f] *Department of Experimental Pathology, Institut d'Investigacions Biomèdiques de Barcelona (IIBB), CSIC-IDIBAPS, Rosselló, 161, 08036 Barcelona, Spain*
[g] *Barcelona Hepatic Hemodynamic Laboratory, Liver Unit, Hospital Clínic, Clínic Barcelona, Health Care Provider of the European Reference Network on Rare Liver Disorders (ERN-RareLiver), CSUR Centro de Referencia del Sistema Nacional de Salud en Enfermedad Hepática Vascular Compleja en adultos, Barcelona, Spain*
[h] *Fundació de Recerca Clínic Barcelona-Institut d'Investigacions Biomèdiques August Pi i Sunyer (FRCB-IDIBAPS), Barcelona, Spain*
[i] *Centro de Investigación Biomédica en Red Enfermedades Hepáticas y Digestivas (CIBEREHD), Madrid, Spain*
[j] *Medicine Department, Faculty of Medicine, and Health Science, Universitat de Barcelona, Barcelona, Catalonia, Spain*
[k] *Cardiovascular Institute, Hospital Clinic, Institut d'Investigacions Biomèdiques August Pi i Sunyer (IDIBAPS), University of Barcelona, 08036 Barcelona, Spain*
[l] *Hematopathology, Centre Diagnòstic Biomèdic (CDB), Hemotherapy-Hemostasis Department, Hospital Clinic, Institut d'Investigacions Biomèdiques August Pi i Sunyer (IDIBAPS), University of Barcelona, 08036 Barcelona, Spain*
[m] *Barcelona Endothelium Team (BET), 08036 Barcelona, Spain*
[n] *BCNatal|Fetal Medicine Research Center, Hospital Clínic and Hospital Sant Joan de Déu, Institut d'Investigacions Biomèdiques August Pi i Sunyer (IDIBAPS), University of Barcelona, 08036 Barcelona, Spain*
[o] *Centre for Biomedical Research on Rare Diseases (CIBER-ER), Instituto de Salud Carlos III, 28029 Madrid, Spain*
[p] *Department of Biological Sciences, Faculty of Science, University of Girona, 17003 Girona, Spain*

ARTICLE INFO

Article history:
Received 9 October 2025
Accepted 28 August 2026
Available online xxx

Keywords:
Endothelial dysfunction
Chronic thromboembolic pulmonary hypertension
Transcriptomic profile
Translational and ribosomal dysregulation

ABSTRACT

Objectives: Pulmonary arterial hypertension (PAH) and chronic thromboembolic pulmonary hypertension (CTEPH) are rare, severe forms of pulmonary hypertension (PH) characterized by elevated mean pulmonary arterial pressure (mPAP) and ~20% mortality at 3 years. PAH is defined by progressive obliterative vasculopathy, whereas CTEPH results from persistent pulmonary artery obstruction by fibrotic thrombotic material, leading to vascular remodelling, right ventricular hypertrophy, and heart failure.
Methods: Endothelial colony-forming cells (ECFCs) derived from PAH and CTEPH patients and healthy-controls were analysed to identify disease-specific molecular and functional alterations. Transcriptomic profiling was integrated with functional assays, including global protein synthesis, mitochondrial bioenergetics, intracellular Ca^{2+} dynamics, and cellular ultrastructural assessment by transmission electron microscopy (TEM). The effects of riociguat, the approved therapy for inoperable or persistent post-surgical CTEPH, were also evaluated.

Abbreviations: PAH, pulmonary arterial hypertension; CTEPH, chronic thromboembolic pulmonary hypertension; PH, pulmonary hypertension; mPAP, mean pulmonary arterial pressure; ECFCs, endothelial colony-forming cells; TEM, transmission electron microscopy; BMPR2, bone morphogenetic protein receptor type 2; PEA, pulmonary endarterectomy; RPL, ribosomal protein large subunit proteins; RPS, ribosomal protein small subunit; MNC, human mononuclear cells; DEGs, differentially expressed genes; GO, gene ontology; FEV_1/FV, spirometry volumes ratio; WHO-FC, world functional class; ER, endoplasmic reticulum; MAM, endoplasmic reticulum membranes.

* Corresponding authors.
E-mail addresses: mperacaula@idibgi.org (M. Peracaula), jbarbera@clinic.cat (J.A. Barberà), olgaturac@gmail.com (O. Tura-Ceide).

https://doi.org/10.1016/j.arbres.2026.08.018
0300-2896/© 2026 The Authors. Published by Elsevier España, S.L.U. on behalf of SEPAR. This is an open access article under the CC BY-NC-ND license (http://creativecommons.org/licenses/by-nc-nd/4.0/).

Please cite this article as: M. Peracaula, D. Aguilar, À. Vea et al., Endothelial Cell Transcriptomics Reveal Activation of Ribosomal-related Pathways in Chronic Thromboembolic Pulmonary Hypertension, Archivos de Bronconeumología, https://doi.org/10.1016/j.arbres.2026.08.018

Results: Significant differences in gene expression profiles were observed among PAH-ECFCs, CTEPH-ECFCs, and control-ECFCs. CTEPH-ECFCs, exhibited a unique upregulation of ribosomal and translation-related genes, accompanied by increased global protein synthesis. Network analysis revealed a highly connected ribosomal–translational hub within CTEPH transcriptome signature. CTEPH-ECFCs also exhibited mitochondrial remodelling, increased endoplasmic reticulum–mitochondria contacts, altered intracellular Ca^{2+} handling, and reduced maximal respiratory capacity. Riociguat did not reverse these abnormalities.

Conclusions: Dysregulated protein biosynthesis is a characteristic feature of CTEPH, distinguishing them from PAH. Our findings highlight a coordinated translation–mitochondria–MAM axis potentially involved in endothelial dysfunction and vascular remodelling, supporting the need for therapies targeting disease-specific molecular pathways beyond soluble guanylate cyclase stimulation.

© 2026 The Authors. Published by Elsevier España, S.L.U. on behalf of SEPAR. This is an open access article under the CC BY-NC-ND license (http://creativecommons.org/licenses/by-nc-nd/4.0/).

Introduction

Pulmonary hypertension (PH) is a medical condition with abnormal increase in mean pulmonary arterial pressure (mPAP) >20 mmHg at rest [1]. Within PH, pulmonary arterial hypertension (PAH) and chronic thromboembolic pulmonary hypertension (CTEPH) are rare subtypes [1,2]. PAH has an estimated prevalence of 2.6 per 100,000 inhabitants, while CTEPH affects approximately with 1.1 per 100,000 inhabitants [3,4]. Both conditions are associated with progressive vascular remodelling, elevated pulmonary artery pressures, and right ventricular failure, leading to poor survival with mortality ~20% within three years despite therapeutic advancements [5].

PAH is a severe progressive PH form with narrowing, thickening, and stiffening of small lung arteries [1,3]. This remodelling increases resistance to blood flow, raising pulmonary arterial pressure [1,2,6]. Increased pressure strains the right heart, causing hypertrophy, failure, and death. On the other hand, CTEPH is characterized by persistent obstruction of pulmonary arteries by fibrous thrombotic material. This material attaches to the intimal layer, followed by pulmonary vascular remodelling causing narrowing and occlusion of the vessel lumen [1,3,4]. In nearby non-occluded vessels, an arteriopathy similar to PAH can develop, crucial for determining effectiveness of surgical treatments. Pathogenesis of CTEPH, particularly mechanisms of thrombus formation, resolution failure, and peripheral vasculopathy, remains poorly understood [7].

Dysregulation of vascular tone and endothelial cell proliferation plays a critical role in onset and progression of PAH and CTEPH [1,3,8]. Evidence indicates that both the presence and extent of endothelial dysfunction correlate with PH severity and strongly predict severe complications [1,2,8]. Recent research has focused on molecular pathways underlying endothelial dysfunction, vascular remodelling, and abnormal cell proliferation, all of which are central to PH pathogenesis. Although several approved vascular-targeted therapies are currently used, including sildenafil, bosentan, or sotatercept for PAH and riociguat for inoperable or residual PH in CTEPH, and can improve blood flow, quality of life, exercise capacity, and slowing disease progression, they do not cure the disease [9–11]. There remains an urgent need to identify novel molecular targets and signalling pathways involved in endothelial dysfunction to support the development of new therapies. Deeper mechanistic understanding will accelerate discovery of precision treatments and enable improved diagnostics and personalized PH management.

Direct access to vascular tissue in living patients is challenging. Circulating late-outgrowth endothelial progenitor cells (ECFCs) from peripheral blood, which lack hematopoietic markers and closely resemble mature endothelial cells, offer a non-invasive alternative for assessing patients' endothelial function and serve as biomarkers of vascular health [12]. These cells mobilize in response to vascular injury, differentiate into endothelial cells, and promote neovascularization. By reflecting patient-specific vascular alterations, ECFCs provide an accurate, minimally invasive model for mechanistic studies and therapeutic development [12].

This study aims to investigate the molecular mechanisms underlying endothelial dysfunction in patients with PAH and CTEPH. By analysing the transcriptomic profiles of patient-derived ECFCs and comparing them with those from healthy controls, we seek to define disease-specific expression signatures. We hypothesize that PAH- and CTEPH-derived ECFCs exhibit distinct transcriptomic landscapes, which may reveal dysregulated molecular pathways and highlight potential targets for novel diagnostic biomarkers and personalized therapeutic strategies.

Materials and methods

An expanded version is available in the Data Supplement.

Study population

This case–control study included patients with PAH and CTEPH diagnosed according to current guidelines [1] between 2016 and 2017. Patients with CTEPH underwent pulmonary endarterectomy (PEA) at the Hospital Clinic of Barcelona, Spain. Patient characteristics are summarized in Table 1, and inclusion and exclusion criteria are provided in the Supplementary Material.

Ethics statement

All procedures followed institutional and national ethical standards and the 1964 Helsinki Declaration. Ethics approval was granted by the Hospital Clínic of Barcelona (HCB/2015/0585). Written informed consent was obtained from all participants.

Endothelial progenitor cell isolation

ECFCs were isolated from peripheral blood mononuclear cells via Ficoll-Paque centrifugation and cultured on type I collagen-coated plates [12]. Colonies were counted upon appearance. After quality control, 16 ECFC lines were included: 4 controls, 7 PAH, and 5 CTEPH.

RNA isolation and transcriptomic analysis

Total RNA was purified from ECFCs with RNeasy Mini kit (Qiagen, Hilden, Germany). Only samples with RNA concentration >100 ng/μL, 260/280 ratio >1.8, and RIN >8 were included.

RNA samples were hybridized to GeneChip™ Human Gene 2.1 ST Array Plates (Thermo Fisher, Waltham, MA, USA), detecting >30,000 mRNA and 10,000 lincRNA/miRNA transcripts. Data were normalized using Robust Multi-array Average (RMA) method.

Table 1
Clinical parameters, lung function and laboratory measurements collected from PH, CTEPH and PAH patients. All values expressed as mean ± SD.

Variables	CL $n=4$	PH $n=12$	PAH $n=7$	CTEPH $n=5$
Age, years	46.2 ± 6.9	56.3 ± 15.5	48.3 ± 18.4	68.4 ± 11.9*
Male sex, n (%)	1 (25%)	9 (75%)	5 (71.4%)	4 (80%)*
BMI (kg/m²)	24.8 ± 2.0	25.2 ± 4.5	24.6 ± 3.8	26.0 ± 5.7
Current smoker	0 (0%)	2 (16.6%)	0 (0%)	2 (40%)
Ex-smoker	0 (0%)	4 (33.3%)	2 (28.6%)	2 (40%)
FVC (% predicted)	N/A	79.8 ± 18.3	85.7 ± 17.0	74.0 ± 19.7
FEV_1 (% predicted)	N/A	71.6 ± 18.8	73.0 ± 19.8	70.2 ± 17.9
FEV_1/FVC (%)	N/A	81.3 ± 13.5	66.0 ± 8.1	96.7 ± 18.9
TLC (% predicted)	N/A	94.9 ± 13.8	92.3 ± 13.4	97.5 ± 14.2
DLco (% predicted)	N/A	54.4 ± 18.6	54.9 ± 18.7	54.0 ± 18.6
DLCO/VA	N/A	63.9 ± 14.9	65.8 ± 14.5	62.0 ± 15.4
SvO_2 (%)	N/A	63.6 ± 7.4	64.7 ± 5.0	62.6 ± 9.9
mPAP (mmHg)	N/A	47.8 ± 10.2	50.3 ± 7.7	45.4 ± 5.7
PAWP (mmHg)	N/A	7.8 ± 2.2	8.1 ± 1.2	7.6 ± 3.2
RAP (mmHg)	N/A	8.5 ± 4.8	7.5 ± 4.8	9.6 ± 8.8
CI (L/min/m²)	N/A	2.2 ± 0.3	2.0 ± 0.4	2.4 ± 0.3
6MWT (m)	N/A	432.9 ± 120.3	484.0 ± 113.4	381.8 ± 127.3
PVR (dyn s cm⁵)	N/A	905.4 ± 181.5	1069 ± 265.5	747.2 ± 97.6
BNP (pg/ml)	3.4 ± 4.4	201.2 ± 82.7	254.4 ± 46.3	148.0 ± 119.1
WHO FC, n (%)				
I	N/A	2 (16.7%)	2 (28.6%)	0 (0%)
II		5 (41.7%)	5 (71.4%)	0 (0%)
III–IV		5 (41.7%)	0 (0%)	5 (100%)

Data are shown as mean ± SD. PAH: pulmonary arterial hypertension; CL: healthy controls; CTEPH: chronic thromboembolic pulmonary hypertension; BMI: body mass index, FVC: forced vital capacity; FEV_1: forced expiratory volume in the first second; FEV_1/FVC: ratio of forced expiratory volume in 1 s; TLC: total lung capacity; DLco: diffusing capacity of the lung for carbon monoxide; DLCO/VA: diffusing capacity divided by the alveolar volume; SvO_2: venous oxygen saturation; mPAP: mean pulmonary arterial pressure; PAWP: pulmonary artery wedge pressure; RAP: right atrial pressure; CI: cardiac index; 6MWT: 6 minute walk test; PVR: pulmonary vascular resistance; BNP: brain natriuretic peptide; WHO FC: functional class world health organization; N/A: not applicable.
* $p < 0.05$ CTEPH-ECFC compared to controls-ECFC.

Differential expression analysis

Using R software, differentially expressed genes (DEGs) were identified with the RankProd package ($|\log2FC| > 0.585$, adj. $p < 0.05$) [13–15]. Comparisons included: PAH vs controls, CTEPH vs controls, and CTEPH vs PAH. Differential gene expression between groups was also assessed using the *Limma* package to validate and complement the results obtained with RankProd.

Functional annotation

Gene ontology (GO) *biological process* and *cellular component* terms [16,17] were analysed using *BinoX* and *rrvgo* [18]. Only annotations with experimental evidence codes were considered. Detailed term assignments are in Supplementary File S1.

Interactomic analysis

Protein interaction networks were built using Reactome and STRING databases, visualized with Cytoscape.

RT-qPCR and western blot

Validation of selected genes was performed using RT-qPCR and western blot on independent ECFC cohorts (Supplementary Table 1). Gene expression was normalized to β-actin ($2-\Delta\Delta Ct$ method). Primer sequences and primary antibodies are listed in Supplementary Tables 2 and 3.

Protein synthesis assay

Global protein synthesis in endothelial cells was measured using the protein synthesis assay kit (Red, Abcam) based on O-propargyl-puromycin (OPP) incorporation. Cells were incubated with OPP, and fluorescence was detected by microscopy after DAPI staining. Data are reported as arbitrary units (AU) and represent the mean of biological replicates.

Transmission electron microscopy (TEM)

ECFCs were fixed, embedded, sectioned, stained, and imaged using a JEOL JEM 1010 microscope. Mitochondrial and ultrastructural features were quantified using Fiji software [19] (ImageJ-based) following the Lam et al., 2021 protocol [20].

Seahorse XF mitochondrial stress test

Mitochondrial respiration was assessed using the Seahorse XFe96 Analyzer (Agilent Technologies). Oxygen consumption rate (OCR) was measured under basal conditions and following sequential injection of oligomycin, FCCP, and rotenone/antimycin A. OCR values were normalized to cell number and expressed as pmol O_2/min/10^4 cells.

Intracellular Ca^{2+} measurement

Basal intracellular calcium levels in ECFCs were assessed using the Fluo-4 Calcium Fluorometric Assay Kit (Elabscience) and measured in a microplate reader (Ex/Em 490/525 nm). Fluorescence intensity was normalized to cell number. For selected experiments, riociguat (20 μM, 24 h) was applied to evaluate its effect on calcium handling. A detailed protocol is provided in the Supplementary Material.

Riociguat treatment

CTEPH and control ECFCs were treated with 20 μM riociguat for 24 h, based on prior dose optimization [21]. Post-treatment, RT-qPCR and TEM were repeated to assess effects on translation-related genes and ultrastructural features.

Correlation analysis

Partial correlation analyses adjusted for age and sex were performed in the validation cohort to assess associations between ribosomal gene expression and clinical parameters. Analyses were conducted both at the individual gene level and by grouping genes into RPL and RPS families. Correlation matrices were visualized as heatmaps, and selected significant relationships were further explored using scatter plots.

Statistic analysis

GraphPad Prism 8.0 was used. Data are presented as mean ± SD. *t*-Test or Mann–Whitney *U* for two groups; one-way ANOVA with Tukey's or Kruskal–Wallis with Dunn's post-hoc for multiple comparisons. $p \leq 0.05$ was considered significant.

Data availability

All data are available as Supplementary Material.

Results

Patient demographic analysis and ECFCs characterisation

Twelve patients with pulmonary hypertension (seven with idiopathic PAH and five with CTEPH) and four controls matched for age and BMI were included. To minimize confounding, age and sex were included as covariates in the Limma-based transcriptomic analysis (see Supplementary Material). Patients with PAH had a lower FEV1/FVC ratio and higher mean pulmonary arterial pressure (mPAP) and pulmonary vascular resistance (PVR) than patients with CTEPH (Table 1). However, while patients with PAH were classified as World Health Organization functional class (WHO-FC) I or II, all patients with CTEPH were classified as WHO-FC III. Invasive measurements, such as those obtained by right heart catheterization, were not available for control subjects.

Isolated ECFCs showed high expression of canonical endothelial markers (e.g., VWF, CDH5, KDR) and low to absent expression of hematopoietic markers (CD45, CD68) confirming endothelial purity (Supplementary Table 3), consistent with our previous publications [12]. This findings were further supported by immunofluorescence and RT-qPCR analyses showing expression of endothelial proteins (CD31, vWF, VE-CAD, eNOS) in ECFCs but not in smooth muscle controls (Supplementary Fig. 1).

Transcriptomic profiling identifies distinct gene expression signatures in PAH-ECFCs and CTEPH-ECFCs

A total of 121 differentially expressed genes (DEGs) were found between CTEPH-ECFC *versus* control-ECFC (96 up-regulated, 25 down-regulated), 48 DEGs were found between PAH-ECFCs *versus* control-ECFCs (42 up-regulated, 6 down-regulated). The comparison between CTEPH-ECFCs *versus* PAH-ECFCs showed 413 DEGs (246 up-regulated, 167 down-regulated), indicating substantial transcriptomic divergence between these two diseases identities. The most significantly dysregulated genes for each comparison are presented in Supplementary Fig. 2A, while the complete DEG lists, including log2 fold changes and adjusted *p*-values, are provided in Supplementary File S2.

Functional enrichment analysis identifies translational pathways as a dominant signature in CTEPH ECFCs

An interactome-based functional analysis of the DEGs was performed using gene ontology (GO). The DEGs were separated into up-regulated and down-regulated categories. Fig. 1A shows functional annotation of *biological process* ontology for all DEGs, classified into broad functional categories (complete results are available as Supplementary File S3), while functional annotations of *cellular component* ontology for all DEGs are presented in Fig. 1B, classified into broad functional categories (complete annotation can be found in Supplementary File S4).

The functional categories most associated with PAH-ECFCs (indicated by blue arrows in Fig. 1A and B) comprised immune response, cytoskeletal remodelling, proliferation and differentiation, migration, cytokine pathways, protein activity, and lipid metabolism, aligned with findings from previous studies [22–24].

The functional categories most associated with CTEPH-ECFCs (indicated by red arrows in Fig. 1A and B) included mRNA catabolic process, translation, RNA processing, cytosolic large ribosomal subunit, cytosolic small ribosomal subunit and polysome. These functional categories were uniquely overexpressed in the CTEPH-ECFCs in both comparisons: CTEPH-ECFCs versus PAH-ECFCs and CTEPH-ECFCs versus control-ECFCs, with no evidence in PAH nor control groups. To our knowledge, these findings represent the first report of a translationally enriched transcriptomic signature in CTEPH-ECFCs, suggesting a previously unrecognized molecular feature of the disease.

Network analysis highlights a ribosomal translation hub in CTEPH ECFCs

To further explore the functional relationships among DEGs associated with translational pathways, interactome-based network analysis was performed. DEGs within the interactome of genes belonging to the *translation* functional category were shown in Fig. 2. Fig. 2 illustrates the genes related to *translation* (circled with purple) plus DEGs directly connected to them (no purple circle) in the interactome. Genes up-regulated in CTEPH-ECFCs *versus* controls-ECFCs are visibly connected to *translation*-related genes and were mostly localized within the densely interconnected area composed of ribosomal proteins. These genes also tended to have larger node sizes, indicating higher connectivity in the network. Conversely, down-regulated genes were mainly found in areas of low connection density in the fringes of the interactome. Because the connectivity of a gene product is closely linked to its functional relevance, this figure not only confirms the role of *translation* upregulation in CTEPH-ECFCs but also serves as a visual aid for identifying the most significant DEGs. Additionally, when mapping the DEGs from CTEPH-ECFCs *versus* PAH-ECFCs onto the *translation* interactome (Fig. 2C), a clear upregulation of the *translation* related gene network emerges with central bigger nodes. In contrast, the DEGs in PAH-ECFCs *versus* control-ECFCs exhibit only marginal connections to translation-related genes, as indicated by their smaller nodes (Fig. 2B).

Together, these results identify a highly connected ribosomal translation module as a central feature of the CTEPH-ECFC transcriptome. For clarity, zoomed-in versions are provided in Supplementary Figs. 3–5.

Translation-related gene expression in CTEPH ECFCs

Based on the transcriptomic and network analyses, the most highly connected translation-related genes were selected for further validation by *Limma* package, adjusting for sex and age (Supplementary Fig. 2B). These included ribosomal protein genes such as members of RPS and RPL family and the proto-oncogene FOS. All these genes encode ribosomal proteins except for *FOS*, which encodes for transcriptional regulatory protein. Their expression levels were first examined in the transcriptomic dataset (Fig. 3A). Several ribosomal genes, including *RPS2*, *RPL23*, *RPL23A*, *RPL21*, *RPL12*, *RPSA* and *RPL32*, showed particularly strong upregulation in CTEPH-ECFCs compared with both PAH-ECFCs and control-ECFCs.

Further validation was carried out by RT-qPCR using an independent cohort of CTEPH-ECFCs obtained from a separate set of patients matched for age and sex (Fig. 3B). Consistent with the transcriptomic data, all translation-related genes analysed (*RPS2*, *RPL23*, *RPL4*, *RPL21*, *RPSA*, *RPL32*) were significantly overexpressed in CTEPH-ECFCs compared with control-ECFCs. In contrast, FOS expression was consistently downregulated in both transcriptomic and RT-qPCR analyses. Protein-level validation was subsequently performed by western blotting for representative ribosomal proteins. Both RPL32 and RPL23A showed increased protein expression in CTEPH-ECFCs compared with controls (Fig. 3C), confirming the translational signature identified at the transcriptomic level.

Increased protein synthesis in CTEPH ECFCs

To determine whether the observed transcriptional upregulation of ribosomal and translation-associated genes was associated

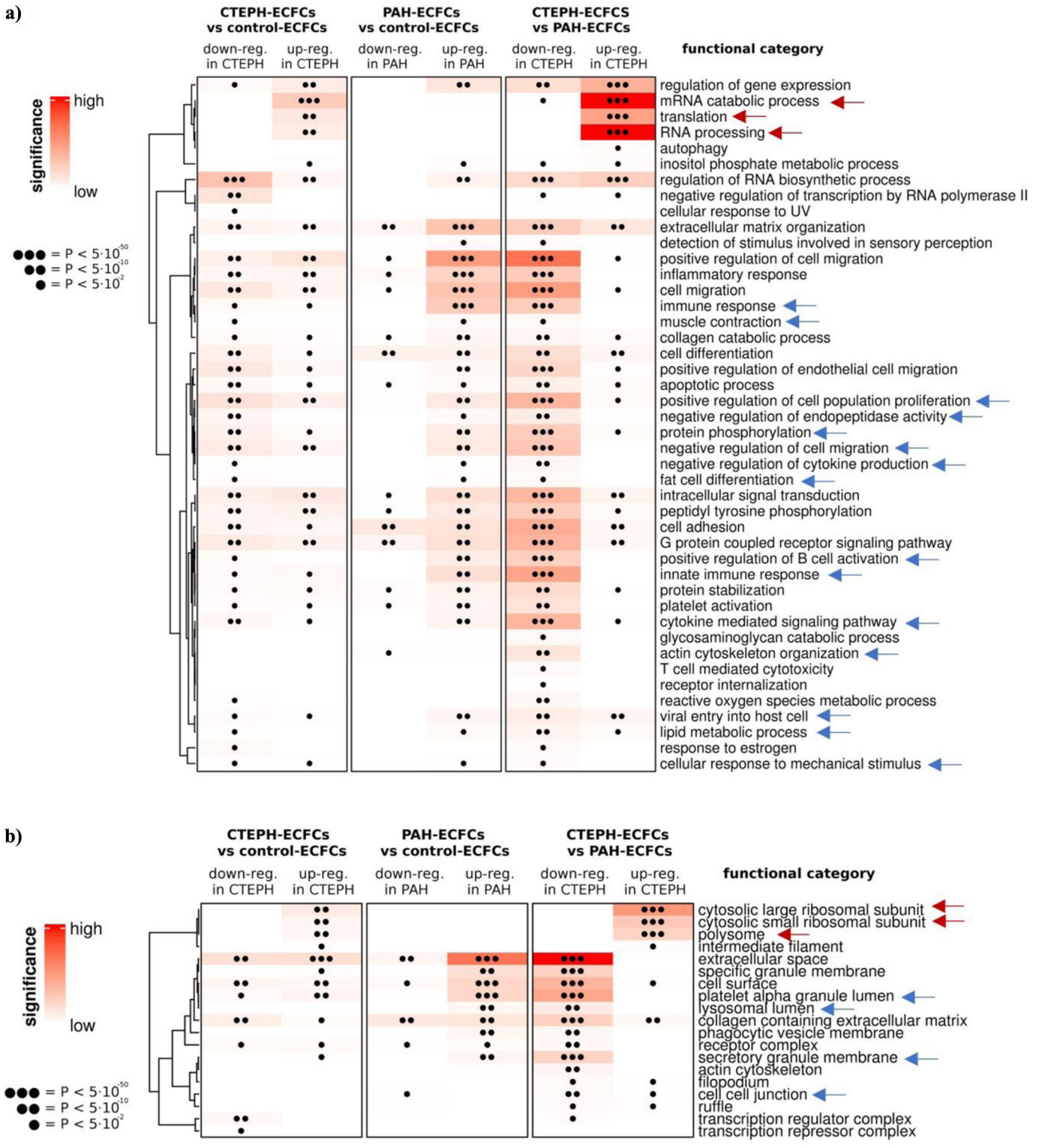

Fig. 1. Functional enrichment analysis of differentially expressed genes in ECFCs. (a) Summary of functional annotation related to *biological process* ontology. (b) Summary of functional annotation and related to *cellular component* ontology. *p*-Values indicated represent the lowest adjusted *p*-value among all GO terms within each functional category. Red arrows indicate the most significant enriched categories in CTEPH-ECFCs ($n = 5$), and blue arrows enriched categories in PAH-ECFCs ($n = 7$), controls-ECFCs ($n = 4$). "*n*" refers to independent biological donors.

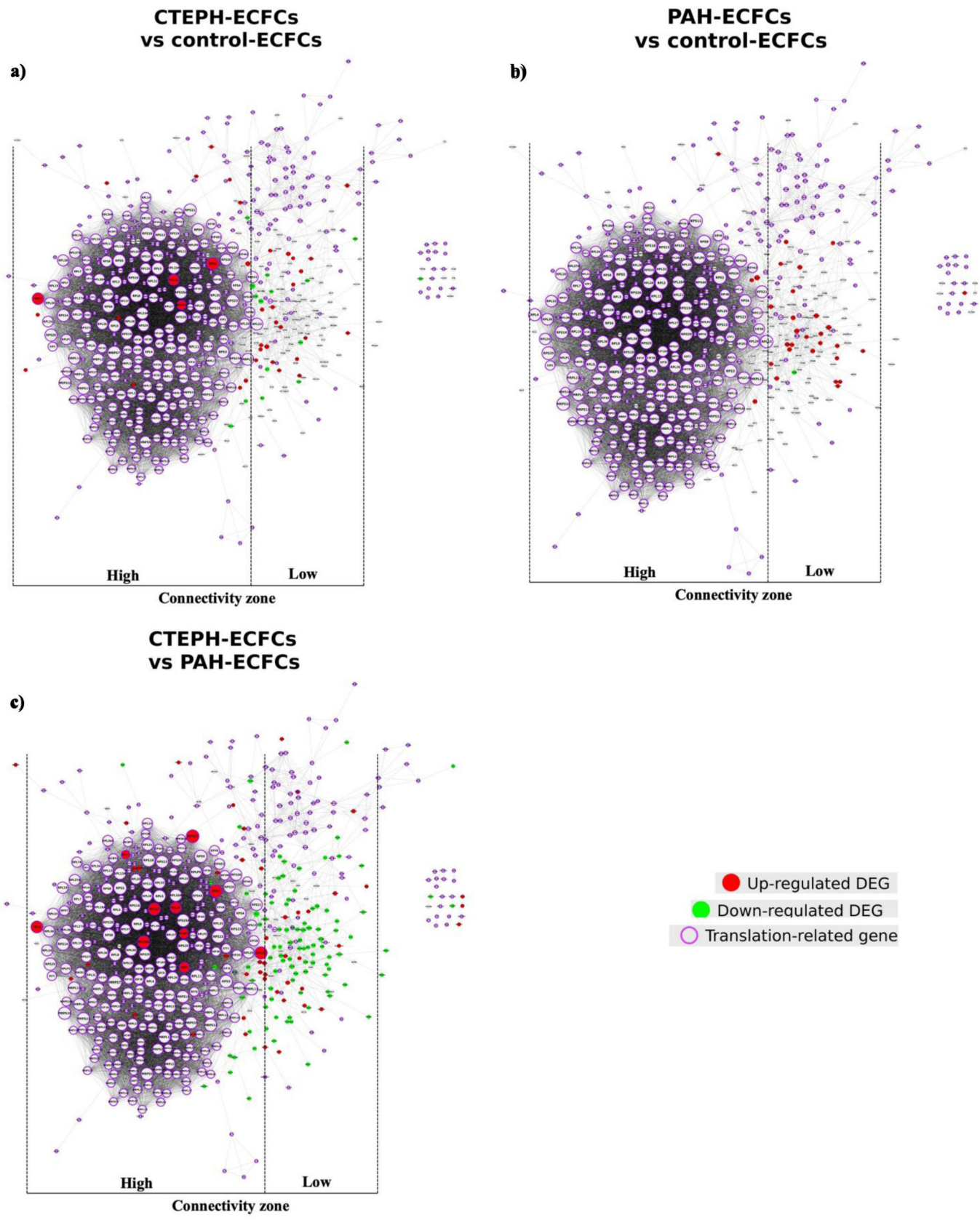

Fig. 2. Connectivity between DEGs and translation. Node size is proportional to connectivity (i.e. the number of neighbors). (a) CTEPH ($n = 5$) compared to control ($n = 4$); (b) PAH ($n = 7$) compared to control; (c) CTEPH compared to PAH. High connectivity area is the grey zone, and low connectivity are is the right white zone. Red nodes indicated up-regulated genes. Green nodes indicate down-regulated genes. Purple border indicates translation-related gene. Each dataset corresponds to independent biological replicates (ECFC donor-derived samples). For zoomable version of this figure, see Supplementary Figs. 3–5.

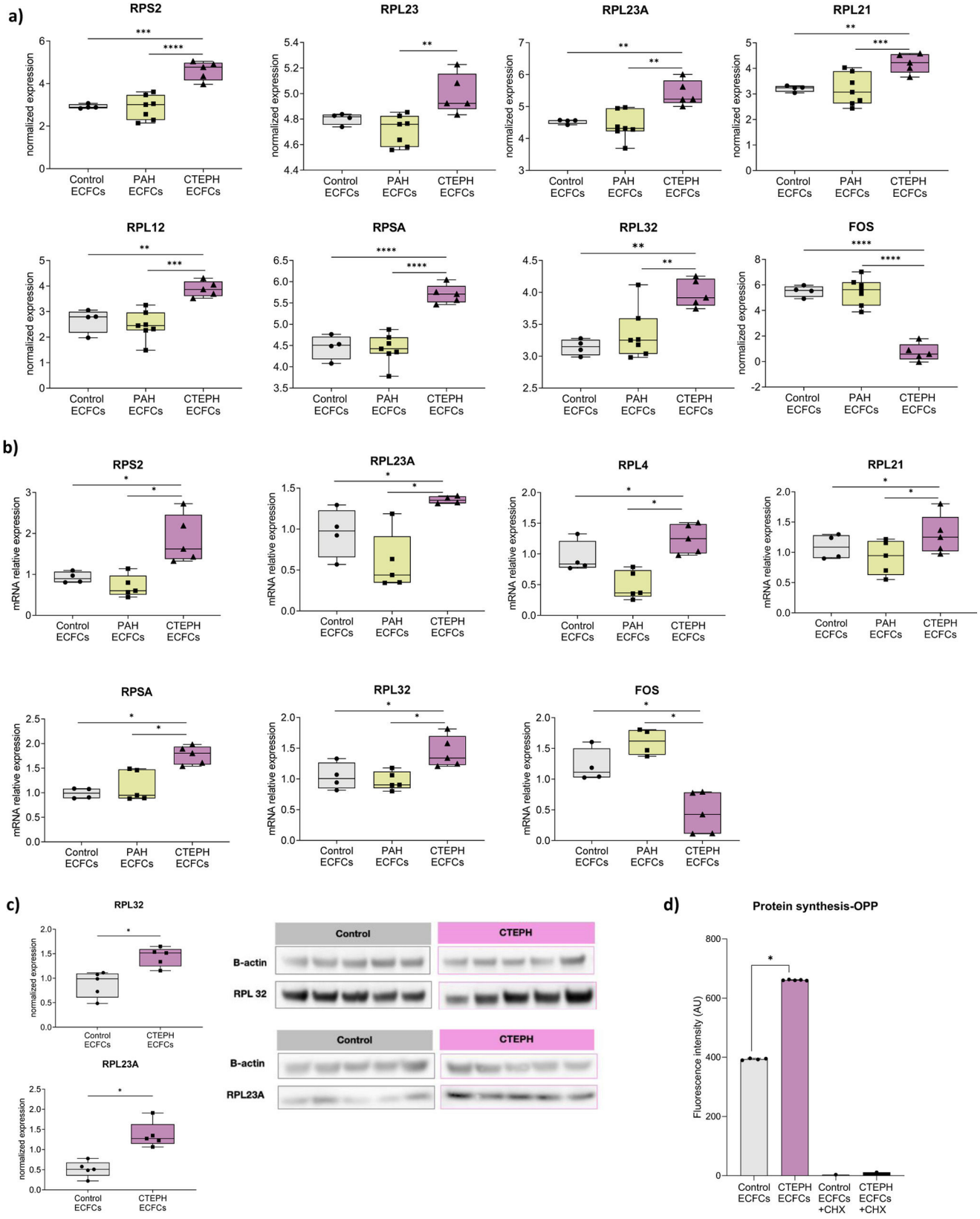

Fig. 3. Translation related gene and protein expression in CTEPH-ECFCs. (a) Expression boxplots for DEGS connected to translation genes in CTEPH-ECFCs ($n = 5$) vs PAH-ECFCs ($n = 7$) vs controls-ECFCs ($n = 4$). (b) Expression boxplots for genes that underwent RT-qPCR validation in CTEPHECFCs ($n = 5$) vs PAH-ECFCs ($n = 5$) vs controls-ECFCs ($n = 4$). The genes selected are the ones that are include in the top most connected to translation category (CTEPH *vs* PAH). Each data point represents an individual biological replicate, with 3 technical replicates per sample, which were averaged prior to statistical analysis. (c) Expression boxplots for RPL32 and RPL23A protein genes that underwent western blot validation. These proteins selected are the ones that are include in the top most connected to translation category genes (CTEPH *vs* PAH). Each point represents an independent biological replicate (donor). (d) Increased protein synthesis in CTEPH-ECFCs. Protein synthesis was assessed in ECFCs from the same donors incubated with OPP. Cycloheximide (CHX) was used as a negative control to block translation. Each data point represents an individual biological replicate, with 3 technical replicates per sample, which were averaged prior to statistical analysis. Statistical analysis was performed using one-way ANOVA followed by Tukey's post-hoc test or the nonparametric Kruskal–Wallis test with Dunn's multiple comparison test (a and b), and *t*-test student (c and d). Significant differences *p*-value *<0.05, **<0.01, ***<0.001, ****<0.0001.

with functional changes in protein production, global protein synthesis was assessed.

CTEPH-ECFCs exhibited significantly increased protein synthesis rates compared with control-ECFCs (Fig. 3D, Supplementary Fig. 6). These findings indicate that the transcriptional activation of translation-related genes is coupled with enhanced translational activity in CTEPH-ECFCs.

TEM analysis reveals alterations in mitochondria-associated endoplasmic reticulum (ER) membranes

Upregulated DEGs associated with the *translation* category include those involved in translocation and elongation pathways, as well as ribosomal subunits. These proteins are directly linked to translational pathways, which relate to the concept of mitochondria-associated endoplasmic reticulum membranes (MAM). This association signifies the physical connection between the ER and mitochondria. Notably, significant alterations in mitochondrial morphology and cristae were observed in CTEPH-ECFCs (Figures 4A). Specifically, mitochondrial roundness (p-value = 0.024), width (p-value = 0.042), and circularity (p-value = 0.008) were significantly reduced in CTEPH-ECFCs compared to controls. The volume (p-value = 0.018) of mitochondrial cristae along with cristae score parameter (p-value = 0.032) were also diminished in CTEPH-ECFCs compared to control-ECFCs (Fig. 4A). To further explore MAM, TEM analysis showed a significant increase in the percentage of mitochondria-ER contact length in CTEPH-ECFCs compared to control-ECFCs (p-value = 0.0004) (Fig. 4A). Representative TEM images are shown in Supplementary Figs. 7 and 8. In line with these structural findings, genes involved in mitochondrial dynamics and mitochondrial quality control, including *PINK1*, *BNIP3L*, *FUNDC1*, and *SQSTM1*, were found to be differentially expressed in our transcriptomic dataset of CTEPH-ECFCs, pointing to disrupted mitochondrial turnover and altered ER–mitochondria stress signalling (Supplementary Fig. 9).

Altered calcium dynamics support MAM remodelling in CTEPH ECFCs

To assess whether the structural alterations observed at ER–mitochondria contact sites had functional consequences, intracellular calcium mobilization was also evaluated. CTEPH-ECFCs displayed altered Ca^{2+} dynamics compared with control-ECFCs. After ATP stimulation, an increase in intracellular Ca^{2+} was observed in both groups, but CTEPH-ECFCs continued to exhibit elevated Ca^{2+} levels, indicating persistent dysregulation of ER–mitochondria calcium communication (Fig. 4B). These results are consistent with the structural remodelling of mitochondria-associated membranes identified by TEM and further suggest that MAM alterations may contribute to the cellular phenotype observed in CTEPH-ECFCs.

Impaired mitochondrial respiratory and mitochondrial translational capacity in CTEPH-ECFCs

To further investigate the functional consequences of mitochondrial remodelling, mitochondrial respiration was assessed in CTEPH-ECFCs and control-ECFCs. CTEPH-ECFCs exhibited an overall reduction in mitochondrial respiratory activity compared with control-ECFCs (Fig. 4C). Specifically, maximal respiration was significantly decreased, indicating reduced oxidative phosphorylation capacity. Basal respiration and ATP-linked respiration were also significantly lower in CTEPH-ECFCs, whereas spare respiratory capacity showed a downward trend that did not reach statistical significance. Proton leak and non-mitochondrial respiration were likewise significantly reduced in CTEPH-ECFCs. Despite these alterations, coupling efficiency remained comparable between groups, suggesting that mitochondrial coupling was preserved despite the overall reduction in respiratory activity.

Consistent with these functional findings, transcriptomic profiling revealed coordinated dysregulation of key oxidative phosphorylation genes in CTEPH-ECFCs, including genes encoding components of complex I (*NDUFS1*, *NDUFS4*, *NDUFS7*, *NDUFA11*), complex II (*SDHC*), and complex IV (*COX4I1*, *COX6B1*, *COX7A2*). These changes were accompanied by concurrent upregulation of cytosolic (*RPL/RPS*) and mitochondrial (*MRPL/MRPS*) ribosomal genes, suggesting enhanced global translational activity and mitochondrial translation capacity (Figs. 3 and 5). Together, these findings suggest that CTEPH-ECFCs adopt a metabolically active state characterised by coordinated nuclear–mitochondrial adaptation, which may support increased biosynthetic demand while partially compensating for impaired respiratory function. Further studies are warranted to clarify the underlying mechanisms and functional significance of these alterations.

Riociguat does not reverse translational or mitochondrial alterations in CTEPH ECFCs

Riociguat treatment did not significantly alter the expression of translation-associated genes (*RPS11*, *RPS2*, *RPL4*, *RPL23A*, *RPSA*, *RPL32*) in either CTEPH-ECFCs or control-ECFCs (Fig. 6A). However, riociguat partially restored FOS expression, which had previously been downregulated in CTEPH-derived cells. Moreover, riociguat had no significant effect on mitochondrial morphology or ER–mitochondria contact length (Fig. 6B). Global protein synthesis also remained unchanged in both CTEPH-ECFCs and control-ECFCs following treatment (Fig. 6C). Similarly, intracellular Ca^{2+} dynamics were unaltered in CTEPH-ECFCs compared with untreated cells (Fig. 6D), and mitochondrial respiratory parameters remained unchanged after treatment (Fig. 6E).

The selected riociguat concentration was based on dose–response analyses (Supplementary Fig. 10) and is supported by previously reported data (Supplementary Material).

Association between ribosomal gene expression and clinical parameters in CTEPH-ECFCs

Significant associations were identified between ribosomal gene expression and clinical and hemodynamic variables in the validation cohort. At both family (RPL/RPS) and individual gene levels, ribosomal expression was positively correlated with leukocyte counts, as well as cardiac output (Qt), cardiac index (CI), and parameters of pulmonary and cardiac function (Supplementary Fig. 11). The strongest associations were visualized using scatter plots (Supplementary Fig. 11).

Discussion

This study provides a comprehensive characterization of molecular and functional alterations in CTEPH- ECFCs, revealing a disease-specific signature that distinguishes them from PAH and healthy ECFCs. CTEPH-ECFCs exhibit a robust upregulation of ribosomal and translation-associated genes independent of sex and age. This transcriptional signature was reinforced by functional evidence of increased global protein synthesis, demonstrating that the molecular changes identified at the transcriptomic level translate into a biologically meaningful enhancement of translational activity. Notably, this signature was not observed in PAH-ECFCs, pointing to a CTEPH-specific adaptive mechanism that may sustain elevated protein production in the context of chronic thromboembolic stress.

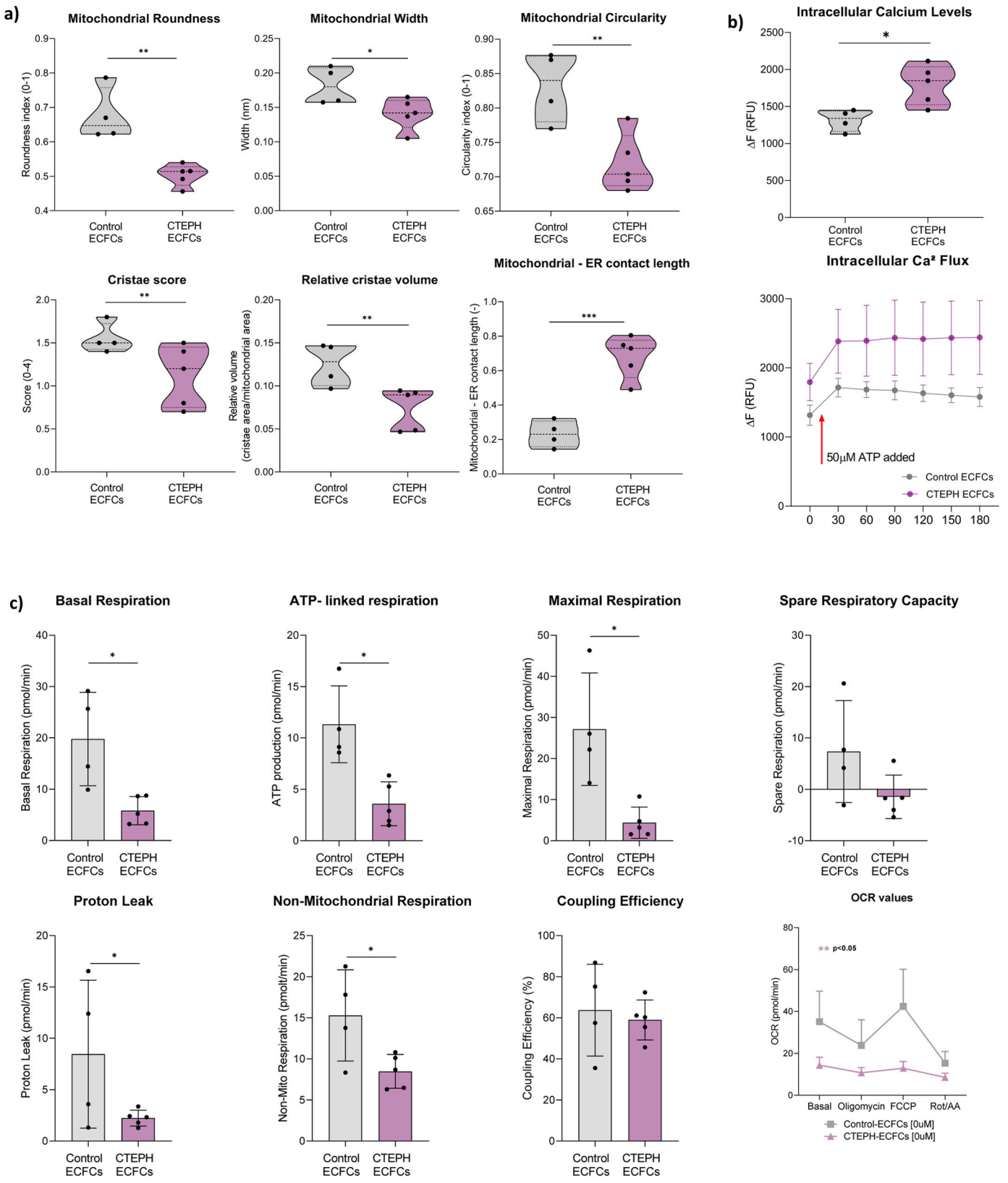

Fig. 4. Mitochondrial morphology, intracellular calcium dynamics, and mitochondrial respiration in control-ECFCs and CTEPH-ECFCs. (a) Transmission electron microscopy (TEM) analysis of mitochondrial ultrastructure. Quantification of mitochondrial morphology (roundness, width, circularity), cristae density, and mitochondria–endoplasmic reticulum (ER) contacts. Each data point represents an independent biological replicate (ECFC donor). Multiple imaging fields were acquired per donor and averaged prior to statistical analysis to avoid pseudoreplication. (b) Intracellular calcium dynamics measured by Fluo-4 AM fluorescence. Basal calcium levels, calcium flux following ATP stimulation are shown. Each data point represents an individual biological replicate (ECFC donor). For each sample, three technical replicates were performed and averaged prior to statistical analysis. ATP dose–response curves are shown in Supplementary Fig. 10. (c) Mitochondrial respiration parameters assessed by Seahorse XF. Measurements were performed in 3 technical replicates per biological replicate and averaged per donor prior to statistical analysis. Data represent independent ECFC donors (control: $n = 4$; CTEPH: $n = 5$). Statistical analysis was conducted using Student's t-test ($^*p < 0.05$).

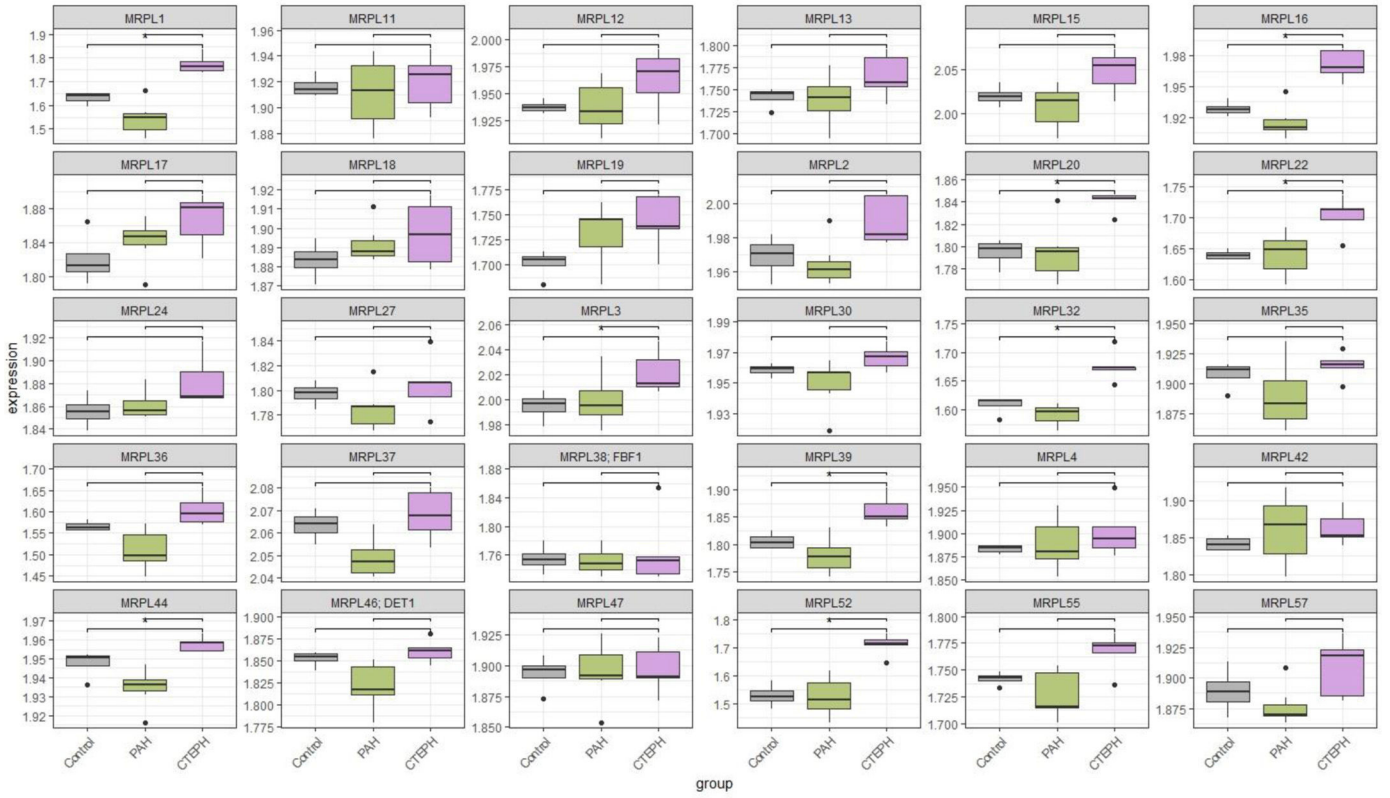

Fig. 5. Expression of MRPL gene family in control, PAH, and CTEPH ECFCs. Boxplots show the distribution of log2-normalized expression values for each MRPL gene. Horizontal lines indicate statistically significant differences compared to CTEPH, determined by Wilcoxon rank-sum test with FDR correction ($p < 0.05$). Each panel represents an individual MRPL gene. Data are derived from independent biological replicates (CTEPH-ECFCs $n = 5$, PAH-ECFCs $n = 7$, control ECFCs $n = 4$).

While PAH is characterized by vascular remodelling driven by inflammation and proliferation, CTEPH arises from persistent vascular obstruction by unresolved thromboembolic material, leading to distinct pathophysiological mechanisms. In line with prior studies, PAH-ECFC transcriptomics showed signatures consistent with endothelial dysfunction such as inflammation, vasoconstriction and proliferation [25,26]. In contrast, dysregulation of translational machinery and ribosomal proteins appeared specific to CTEPH-ECFCs. Our results show a significant upregulation of ribosomal genes, including *RPS2*, *RPL23*, *RPL23A*, *RPL21*, *RPL12*, *RPSA*, and *RPL32* in CTEPH-ECFCs, supporting the notion that these genes may play a key role in maintaining elevated protein synthesis, a mechanism frequently associated with chronic and proliferative diseases [27]. Significantly, this translational program also extended to the mitochondrial compartment, with upregulation of mitochondrial ribosomal and elongation factors such as *MRPL* family, *TUFM*, and *TSFM*, suggesting a potential coordinated enhancement of cytosolic and mitochondrial protein synthesis. This interpretation is consistent with our previous findings of a hyperproliferative phenotype in CTEPH-derived endothelial cells isolated from pulmonary endarterectomy specimens [28–30], as well as with evidence of global proteomic reprogramming obtained by unbiased mass spectrometry, further supporting the biological relevance of this translational signature [31]. These findings also support the premise that peripheral blood–derived ECFCs from patients with CTEPH may recapitulate some salient features of tissue-derived endothelial cells from CTEPH, although direct and systematic comparative studies are required to delineate the extent of this overlap.

Beyond its association with proliferation, the observed translation activation in CTEPH may also be linked to metabolic adaptation. Persistent pulmonary vascular obstruction is expected to impose hypoxic and bioenergetic pressure, and increased translational activity may therefore support the biosynthetic demands associated with endothelial remodelling [32]. In this study, TEM revealed marked mitochondrial ultrastructural abnormalities, including reduced mitochondrial roundness, width, and circularity, together with increased ER–mitochondria contact length, consistent with disrupted mitochondrial dynamics and altered organelle communication [33,34]. These structural alterations were supported by both transcriptomic and functional data. Coordinated dysregulation of oxidative phosphorylation genes, including components of complex I (*NDUFS1*, *NDUFS4*, *NDUFS7*, and *NDUFA11*), complex II (*SDHC*), and complex IV (*COX4I1*, *COX6B1*, and *COX7A2*), was consistent with Seahorse analysis showing reduced basal, maximal, and ATP-linked respiration in CTEPH-ECFCs. Proton leak and non-mitochondrial respiration were also reduced, whereas coupling efficiency remained preserved, suggesting that mitochondrial efficiency is maintained despite overall impaired respiratory activity. Altered expression of genes involved in mitochondrial dynamics and turnover (*DNM1L*, *PINK1*, *BNIP3L*, *FUNDC1*, and *SQSTM1*) further supports the presence of active mitochondrial remodelling. These findings extend our previous observations that CTEPH-derived endothelial cells isolated from pulmonary endarterectomy specimens exhibit mitochondrial dysfunction, oxidative stress, and broader metabolic reprogramming, including reduced glycolytic and glutamine-related pathways [26,28,33,35].

Altered intracellular Ca^{2+} dynamics in CTEPH-ECFCs, together with increased ER–mitochondria contacts, further point to coordinated adaptation across translational, mitochondrial, and MAM-associated pathways. Overall, these data suggest a translation–mitochondria–MAM axis in CTEPH-ECFCs that may sustain endothelial remodelling under chronic thromboembolic stress, although direct functional links between these processes remain to be established [24,36].

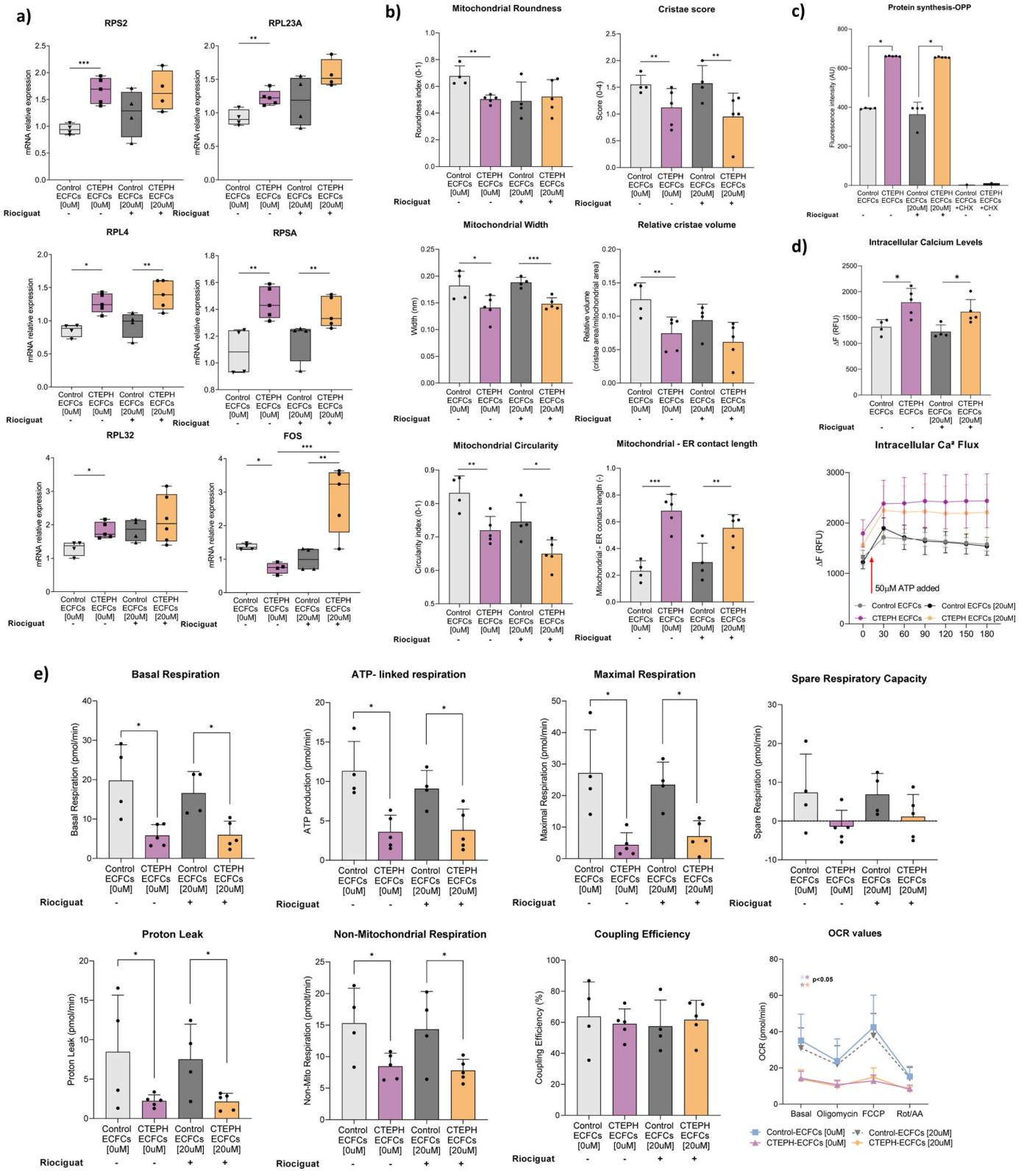

Fig. 6. Effects of riociguat on molecular, metabolic and functional features of control-ECFCs ($n = 4$) and CTEPH-ECFCs ($n = 5$). (a) Relative expression of genes associated with the translation category and the proto-oncogene *FOS* analysed by RT-qPCR in control-ECFCs and CTEPH-ECFCs after treatment with 20 μM riociguat. (b) Ultrastructural analysis of mitochondria from TEM images showing mitochondrial morphology (roundness, width and circularity) and quantification of cristae, and mitochondria–endoplasmic reticulum (ER) contacts in ECFCs ± riociguat treatment. (c) Global protein synthesis assessed by O-propargyl-puromycin (OPP) incorporation in ECFCs incubated ± riociguat, using cycloheximide (CHX) as a negative control to inhibit translation. (d) Functional analysis including intracellular calcium dynamics measured with Fluo-4 AM after ATP stimulation in ECFCs incubated ± riociguat (e) Mitochondrial respiration determined by Seahorse XF analysis (basal respiration, ATP-linked respiration, maximal respiration and spare respiratory capacity) in ECFCs incubated ± riociguat. Each dot represents one biological donor and experiments were performed with three technical replicates unless otherwise indicated. Statistical analyses included Student's *t*-test, one-way ANOVA followed by Tukey's post-hoc test, or the non-parametric Kruskal–Wallis test with Dunn's multiple comparison test as appropriate. Significant differences are indicated as $^{*}p < 0.05$, $^{**}p < 0.01$, $^{***}p < 0.001$.

In addition, correlation analyses showed associations between ribosomal gene expression and clinical parameters, including cardiac index, leukocyte counts and measures of pulmonary and cardiac function. Although limited by sample size, these findings suggest a potential link between the translational signature and hemodynamic status in CTEPH.

Finally, we assessed the potential impact of riociguat, the only approved drug for CTEPH, on the endothelial phenotype identified in this study. Although riociguat is primarily recognized as a vasodilator acting through soluble guanylate cyclase stimulation and cGMP production, it has also been proposed to influence endothelial cell function under specific conditions [21]. However, in our model, riociguat did not reverse the overexpression of translation-associated genes, increased global protein synthesis, mitochondrial and MAM remodelling, calcium dysregulation, or defective mitochondrial respiration in CTEPH-ECFCs. This lack of effect suggests that the translational and metabolic abnormalities identified in CTEPH-ECFCs are not adequately targeted by current vasodilator-based therapy and may require more mechanism-specific therapeutic approaches.

Limitations. This study has several limitations. This study is limited by the relatively small number of biological replicates, which may have reduced statistical power. *In vivo* validation was not performed, largely because well-established animal models of CTEPH are not currently available in our hands and remain the subject of ongoing work. Finally, mechanistic studies incorporating targeted modulation of ribosomal components together with complementary functional assays are needed to establish causality.

In conclusion, our data identify a distinct molecular and functional phenotype in CTEPH-ECFCs defined by enhanced translational activity, mitochondrial remodelling, altered ER–mitochondria communication, calcium dysregulation, and reduced mitochondrial respiratory function. These alterations point to a unique coordinated translation–mitochondria–MAM axis as a potential contributor to endothelial dysfunction and vascular remodelling in CTEPH. The limited impact of riociguat on these abnormalities further highlights the need for therapeutic approaches that directly target the underlying disease-specific endothelial mechanisms.

Authors' contributions

Authors contributions are as follows: O.T.-C. and J.A.B. conceived, designed the study, and supervised the work. H.G.-C., A.P.D., V.H.G., J.C.G.-P., M.D.-R., F.C., designed the methods for the project "Targeting endothelial dysfunction in highly prevalent diseases-PIE15/00027". J.O. and I.B. were involved in recruiting the patients; J.O., and C.R. established the database, collected blood samples, and isolate de cell lines; A.V., J.C.-S. and M.P. performed experimental analysis; M.P., D.A., J.C.-S. and M.G.-A. analysed the data. M.P. and D.A., drafted the manuscript and figures. M.P. and O.T.-C. acquisition of information, writing, and critical revision. V.P., M.P. and O.T.-C. review and editing. All the authors revised the manuscript and approved this submitted final version. All authors have read and agreed to the published version of the manuscript.

Ethical statement

This nested case–control study was part of the project "Targeting endothelial dysfunction in highly prevalent diseases – PIE15/00027". All procedures followed institutional and national ethical standards and the 1964 Helsinki Declaration. Ethics approval was granted by the Hospital Clínic of Barcelona (HCB/2015/0585). Written informed consent was obtained from all participants.

Declaration of generative AI and AI-assisted technologies in the writing process

The authors confirm that no generative artificial intelligence (AI) tools were used in the preparation of this manuscript.

Funding

We gratefully acknowledge the funding institutions: Instituto de Salud Carlos III (PIE15/00027, PI18/00960, PI21/01212, INT21/00027) as part of the National R+D+I Plan, co-financed by ISCIII-Subdirección General de Evaluación and Fondo Europeo de Desarrollo Regional (FEDER) "Una manera de hacer Europa," which enabled the development of this research. Additional support was provided by the Spanish Society of Respiratory Medicine (SEPAR), the Catalan Society of Pneumology (SOCAP), the Spanish Society of Cardiology (SEC/FEC-INV-BAS 23/06), and the Fundación Contra la Hipertensión Pulmonar (FCHP). We also acknowledge that M.P. was funded by a PFIS grant (FI22/00133) from the Instituto de Salud Carlos III, and O.T.-C. received support through Miguel Servet grants from the Instituto de Salud Carlos III (CP17/00114, CPII22/00006), co-funded by the European Social Fund "Investing in Your Future".

Conflict of interests

No conflicts of interest, financial or otherwise, are declared by the authors.

Data availability

The datasets generated and/or analysed during the current study are available from the corresponding author, Dra. Tura-Ceide (olgaturac@gmail.com) on reasonable request.

Acknowledgements

The authors would like to acknowledge Cristina Bonjoch and Keren Lopez for her meticulous technical support. We would also like to express our gratitude to Dra. Rigol and Dra. Solanes for their collaboration and valuable contribution to this work. We thank the TEM-SEM Electron Microscopy Unit from Scientific and Technological Centers (CCiTUB), Universitat de Barcelona, and staff for their support and advice on TEM technique.

Appendix A. Supplementary data

Supplementary data associated with this article can be found in the online version available at https://doi.org/10.1016/j.arbres.2026.08.018.

References

[1] Humbert M, Kovacs G, Hoeper MM, Badagliacca R, Berger RMF, Brida M, et al. 2022 ESC/ERS guidelines for the diagnosis and treatment of pulmonary hypertension. Eur Heart J 2022;43(38):3618–731, http://dx.doi.org/10.1093/eurheartj/ehac237.
[2] Simonneau G, Montani D, Celermajer DS, Denton CP, Gatzoulis MA, Krowka M, et al. Haemodynamic definitions and updated clinical classification of pulmonary hypertension. Eur Respir J 2019;53, http://dx.doi.org/10.1183/13993003.01913-2018, 1801913.
[3] Simonneau G, Dorfmüller P, Guignabert C, Mercier O, Humbert M. Chronic thromboembolic pulmonary hypertension: the magic of pathophysiology. Ann Cardiothorac Surg 2022;11(2):106–19, http://dx.doi.org/10.21037/acs-2021-pte-10.
[4] Leber L, Beaudet A, Muller A. Epidemiology of pulmonary arterial hypertension and chronic thromboembolic pulmonary hypertension: identification of the most accurate estimates from a systematic literature review. Pulm Circ 2021;11(1), http://dx.doi.org/10.1177/2045894020977300, 2045894020977300.

[5] Küçükoğlu MS, Sinan ÜY, Yildizeli B. Ten-year outcome of chronic thromboembolic pulmonary hypertension patients in a tertiary center. Anatol J Cardiol 2020;23(2):105–9, http://dx.doi.org/10.14744/AnatolJCardiol.2019.90329.
[6] Humbert M. Pulmonary arterial hypertension and chronic thromboembolic pulmonary hypertension: pathophysiology. Eur Respir Rev 2010;19(115):59–63, http://dx.doi.org/10.1183/09059180.00007309.
[7] Pepke-Zaba J, Delcroix M, Lang I, Mayer E, Jansa P, Ambroz D, et al. Chronic thromboembolic pulmonary hypertension (CTEPH): results from an international prospective registry. Circulation 2011;124(18):1973–81, http://dx.doi.org/10.1161/CIRCULATIONAHA.110.015008.
[8] McLaughlin VV, Gaine SP, Howard LS, Leuchte HH, Mathier MA, Mehta S, et al. Treatment goals of pulmonary hypertension. J Am Coll Cardiol 2013;62(25):73–81, http://dx.doi.org/10.1016/j.jacc.2013.10.034.
[9] Humbert M, McLaughlin V, Gibbs JSR, Gomberg-Maitland M, Hoeper MM, Preston IR, et al. Sotatercept for the treatment of pulmonary arterial hypertension. N Engl J Med 2021;384(13):1204–15, http://dx.doi.org/10.1056/NEJMoa2024277.
[10] Preston IR, Lewis D, Gomberg-Maitland M. Using sotatercept in the care of patients with pulmonary arterial hypertension. Chest 2024;166(3):604–11, http://dx.doi.org/10.1016/j.chest.2024.06.3801.
[11] Rubin LJ, Badesch DB, Fleming TR, Galiè N, Simonneau G, Ghofrani HA, et al. Long-term treatment with sildenafil citrate in pulmonary arterial hypertension: the SUPER-2 study. Chest 2011;140(5):1274–83, http://dx.doi.org/10.1378/chest.10-0969.
[12] Tura O, Skinner EM, Barclay R, Samuel K, Gallagher RCJ, Brittan M, et al. Late outgrowth endothelial cells resemble mature endothelial cells and are not derived from bone marrow. Stem Cells 2013;31(2):338–48, http://dx.doi.org/10.1002/stem.1280 [cited 8 Jan 2020]. Available from: https://pubmed.ncbi.nlm.nih.gov/23165527/
[13] R Core Team. R: a language and environment for statistical computing [software]. Vienna (Austria): R Foundation for Statistical Computing; 2021 [cited 4 Nov 2023]. Available from: https://www.R-project.org/
[14] Carvalho BS, Irizarry RA. A framework for oligonucleotide microarray preprocessing. Bioinformatics 2010;26(19):2363–7, http://dx.doi.org/10.1093/bioinformatics/btq431.
[15] Del Carratore F, Jankevics A, Eisinga R, Heskes T, Hong F, Breitling R. RankProd 2.0: a refactored bioconductor package for detecting differentially expressed features in molecular profiling datasets. Bioinformatics 2017;33(17):2774–5, http://dx.doi.org/10.1093/bioinformatics/btx292.
[16] Ogris C, Guala D, Helleday T, Sonnhammer ELL. A novel method for crosstalk analysis of biological networks: improving accuracy of pathway annotation. Nucleic Acids Res 2017;45(2), http://dx.doi.org/10.1093/nar/gkw849, e8.
[17] Ogris C, Helleday T, Sonnhammer ELL. PathwAX: a web server for network crosstalk based pathway annotation. Nucleic Acids Res 2016;44(W1):105–9, http://dx.doi.org/10.1093/nar/gkw356.
[18] Supek F, Bošnjak M, Škunca N, Šmuc T. Revigo summarizes and visualizes long lists of gene ontology terms. PLoS One 2011;6(7), http://dx.doi.org/10.1371/journal.pone.0021800, e21800.
[19] Schneider CA, Rasband WS, Eliceiri KW. NIH image to ImageJ: 25 years of image analysis. Nat Methods 2012;9(7):671–5, http://dx.doi.org/10.1038/nmeth.2089.
[20] Lam J, Katti P, Biete M, Mungai M, Ashshareef S, Neikirk K, et al. A universal approach to analyzing transmission electron microscopy with imagej. Cells 2021;10(9):2177, http://dx.doi.org/10.3390/cells10092177.
[21] Poyatos P, Peinado VI, Blanco I, Osorio J, Yuan S, Ramírez AM, et al. Assessing the role of endothelium-protective drugs: functional and molecular insights into chronic thromboembolic pulmonary hypertension derived endothelial cells. Biomed Pharmacother 2025;190, http://dx.doi.org/10.1016/j.biopha.2025.118425, 118425.
[22] Romanoski CE, Qi X, Sangam S, Vanderpool RR, Stearman RS, Conklin A, et al. Transcriptomic profiles in pulmonary arterial hypertension associate with disease severity and identify novel candidate genes. Pulm Circ 2020;10(4), http://dx.doi.org/10.1177/2045894020968531, 2045894020968531.
[23] Ross DJ, Hough G, Hama S, Aboulhosn J, Belperio JA, Saggar R, et al. Proinflammatory high-density lipoprotein results from oxidized lipid mediators in the pathogenesis of both idiopathic and associated types of pulmonary arterial hypertension. Pulm Circ 2015;5(4):640–8, http://dx.doi.org/10.1086/683695.
[24] Pokharel MD, Marciano DP, Fu P, Franco MC, Unwalla H, Tieu K, et al. Metabolic reprogramming, oxidative stress, and pulmonary hypertension. Redox Biol 2023;64, http://dx.doi.org/10.1016/j.redox.2023.102797, 102797.
[25] Haensel M, Wojciak-Stothard B. The role of endothelial cells in pulmonary hypertension: old concepts and new science. Curr Opin Physiol 2023;34, http://dx.doi.org/10.1016/j.cophys.2023.100667, 100919.
[26] Smolders VFED, Rodríguez C, Blanco I, Szulcek R, Timens W, Piccari L, et al. Metabolic profile in endothelial cells of chronic thromboembolic pulmonary hypertension and pulmonary arterial hypertension. Sci Rep 2022;12(1):2283, http://dx.doi.org/10.1038/s41598-022-06238-z.
[27] Ruggero D, Pandolfi PP. Does the ribosome translate cancer? Nat Rev Cancer 2003;3(3):179–92, http://dx.doi.org/10.1038/nrc1015.
[28] Tura-Ceide O, Smolders VFED, Aventin N, Morén C, Guitart-Mampel M, Blanco I, et al. Derivation and characterisation of endothelial cells from patients with chronic thromboembolic pulmonary hypertension. Sci Rep 2021;11(1), http://dx.doi.org/10.1038/s41598-021-98320-1, 18797.
[29] Jia X, He X, Huang C, Li J, Dong Z, Liu K. Protein translation: biological processes and therapeutic strategies for human diseases. Signal Transduct Target Ther 2024;9:44, http://dx.doi.org/10.1038/s41392-024-01749-9.
[30] Zhang G, Wang X, Gillette TG, Deng Y, Wang ZV. Unfolded protein response as a therapeutic target in cardiovascular disease. Curr Top Med Chem 2019;19(21):1902–17, http://dx.doi.org/10.2174/1568026619666190521093049.
[31] Nukala SB, Tura-Ceide O, Aldini G, Smolders VFED, Blanco I, Peinado VI, et al. Protein network analyses of pulmonary endothelial cells in chronic thromboembolic pulmonary hypertension. Sci Rep 2021;11(1):5583, http://dx.doi.org/10.1038/s41598-021-85004-z.
[32] Delcroix M, de Perrot M, Jaïs X, Jenkins DP, Lang IM, Matsubara H, et al. Chronic thromboembolic pulmonary hypertension: realising the potential of multimodal management. Lancet Respir Med 2023;11(9):836–50, http://dx.doi.org/10.1016/S2213-2600(23)00292-8.
[33] Geng Y, Hu Y, Zhang F, Tuo Y, Ge R, Bai Z. Mitochondria in hypoxic pulmonary hypertension, roles and the potential targets. Front Physiol 2023;14, http://dx.doi.org/10.3389/fphys.2023.1239643, 1239643.
[34] Ryanto GRT, Suraya R, Nagano T. Mitochondrial dysfunction in pulmonary hypertension. Antioxidants (Basel) 2023;12(2):372, http://dx.doi.org/10.3390/antiox12020372.
[35] Liang S, Yegambaram M, Wang T, Wang J, Black SM, Tang H. Mitochondrial metabolism, redox, and calcium homeostasis in pulmonary arterial hypertension. Biomedicines 2022;10(2):341, http://dx.doi.org/10.3390/biomedicines10020341.
[36] Sowa G. Caveolae, caveolins, cavins, and endothelial cell function: new insights. Front Physiol 2012;2:120, http://dx.doi.org/10.3389/fphys.2011.00120.